COMPLEX BEHAVIOR IN THE SOURCE PROCESS OF THE 18 AUGUST 2020, BENGKULU, SOUTHWEST OF SUMATRA DOUBLET EARTHQUAKE

Abdul Rosid[1]
MEE20701

Supervisor: Yuji YAGI[2]
Bunichiro SHIBAZAKI[3*], **Tatsuhiko HARA**[3**],
Yushiro FUJII[3**], **Fumio TAKEDA**[4**]

ABSTRACT

This study investigated the source process of the 2020 Bengkulu doublet earthquake (Mw 6.9 and Mw 7.2 by this study) using the high degree of freedom finite fault inversion method recently developed by Shimizu et al. (2020). In the process, we applied some unique treatments by considering an identical fault plane and using the same data set for both earthquakes. Consequently, we have succeeded in reconstructing a reliable interaction of the foreshock and mainshock source processes by showing good waveform fitting between the synthetic waves and the observed waves.

We found that the rupture in the fault plane was divided into two distinct areas between foreshock and mainshock. The foreshock earthquake broke the asperity located in the southeast with a total maximum slip of 1.07 meters, while in the mainshock earthquake, the asperity broke with a total maximum slip of 1.17 meters in the northwest direction. Furthermore, the extension pattern of the 2020 Bengkulu doublet earthquake rupture shows as if the mainshock earthquake continued the unfinished foreshock earthquake rupture but with a more comprehensive area coverage. It seems that the final stage of the foreshock rupture triggered the mainshock hypocenter, which is closely located. Meanwhile, the suspending pattern of the foreshock's and mainshock's rupture extension to the deeper part appears to be related to the 2007 Bengkulu Great Earthquake (Mw 8.5). Moreover, using the high degree of freedom finite fault inversion method, which allows us to extract the fault plane geometry information, we discover that the dip angle changes along the fault plane as the depth increases.

Keywords: doublet earthquake, source process, 2020 Bengkulu earthquake, rupture interaction, trigger.

1. INTRODUCTION

Indonesia is an archipelago country that has quite complicated tectonic conditions. This condition results from a convergence of the world's major plates and several small plates or micro blocks (Bird, 2003). As a result of these conditions, Indonesia also has a high seismic activity every year. Recently, an earthquake with a moment magnitude (Mw) 6.7 (foreshock) occurred in the early morning on 18 August 2020 in the Southwest of Sumatra. According to the Global CMT (https://www.globalcmt.org), the origin time of this earthquake is 22:24:12 UTC and located in 4.56 S, 100.99 E, with a depth of 23 km. Soon after that, another earthquake occurred in almost the exact location with almost the same magnitude. It was Mw 7.0 (mainshock) earthquake that occurred around 5 minutes after the first earthquake. It was located at 4.47 S, 100.86 E, with a depth of 25 km and its origin time is 22:29:38 UTC. By considering the parameters of the two earthquakes, it can be said that this is a twin or doublet

[1] Meteorological, Climatological, and Geophysical Agency (BMKG), Indonesia.
[2] Professor, Department of Life and Environmental Sciences, University of Tsukuba.
[3] International Institute of Seismology and Earthquake Engineering (IISEE), Building Research Institute (BRI).
[4] National Graduate Institute for Policy Studies (GRIPS).
* Chief examiner, ** Examiner

earthquake phenomenon if we refer to Lay and Kanamori (1980). With the doublet earthquake on 18 August 2020, southwest of Sumatra, we will use far-distance seismic broadband records from stations worldwide to conduct a finite fault inversion representing fault deformation on an assumed fault by shear slip vectors by superposition of five basis double couple components to those earthquakes. This method was a new method introduced by Shimizu et al. (2020). In addition, by using the same method, we can extract the geometry information of the subduction slab along the fault plane, which is the source of the doublet earthquake.

2. DATA

In conducting this research, we used teleseismic body-wave data recorded by stations located around the world. Those were downloaded from the official website of Incorporated Research Institutions for Seismology (IRIS; https://ds.iris.edu/wilber3/find_event). By applying several constraints to the teleseismic waveform data, such as the distance range of the stations is 30^o - 90^o from the epicenter (yellow star) (Figure 1), they have a good signal-to-noise ratio in the vertical component, and they must have good azimuthal coverage. We got 54 teleseismic waveforms data recorded from 54 stations worldwide (red triangles) (Figure 1), both for the foreshock and the mainshock.

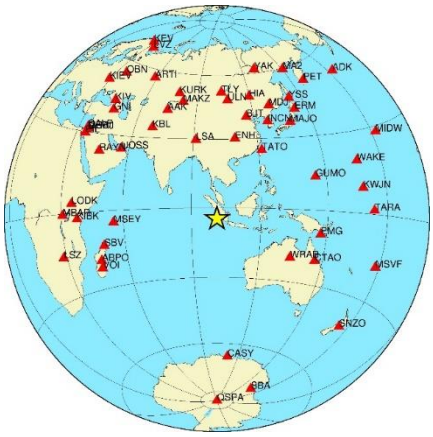

Figure 1. Azimuthal equidistance map view of teleseismic stations which is recording Foreshock and Mainshock.

We deliberately utilized the same dataset for both earthquakes, because considering the fact that both are twin earthquakes which, of course, occurred at almost the exact location and time. Therefore, by downloading the waveforms starting from 1 minute before the P-wave phase of the foreshock to 10 minutes after, we have obtained not only the seismic wave recording data of the foreshock but also the mainshock in only one dataset. The mainshock occurred just 5 minutes after the foreshock. In the condition of a doublet earthquake recording, the P-wave arrival of the second earthquake (mainshock) is hard to identify since it is contaminated by the foreshock wave recording, which is still not over. Consequently, we applied a time-shifted method in determining the P-wave arrival of the mainshock in this study. Once we finish picking the foreshock, we calculate a time difference between the foreshock and mainshock origin time. Then, we employed this time difference to assign the P-wave arrival of the mainshock automatically. This method is not only helpful in solving picking accuracy problems but is also a crucial step in understanding the interaction of a doublet earthquake since we want to infer the mainshock earthquake source parameters based on the foreshock earthquake picking. Furthermore, we referred to the hypocenter and the fault parameter of the doublet earthquake from the Global Centroid Moment Tensor (GCMT; https://www.globalcmt.org), and we assumed the velocity structure based on the 1D model proposed by Collings et al. (2012) since it has the exact location of targeted earthquakes.

3. METHODOLOGY

In investigating the source processes of the doublet earthquake, we implemented a finite-fault inversion that is more flexible than conventional inversion designs. Conventional inverse solutions have been sustained by restricting the model space and reducing the degree of freedom for slip vectors. Nevertheless, these restrictions are not fundamentally physical elements for representing source processes. Furthermore, improper conjectures about the fault geometry can increase modeling errors, produce nonunique final solutions, and make the solutions obtained becomes arduous to interpret (Shimizu et al., 2020). In general, the source of an earthquake can be expressed as the volume moment-rate tensor density $\dot{M}(t,\xi)$ (Backus and Mulcahy, 1976), implied by a linear combination of five basis double couple components M_q (Kikuchi and Kanamori, 1991) as shown by Eq. (1):

$$\dot{\mathrm{M}}(t,\boldsymbol{\xi}) = \sum_{q=1}^{5} \dot{\mathrm{m}}_q\ (t,\boldsymbol{\xi})\ \boldsymbol{M_q} \tag{1}$$

where $\dot{m}_q(t,\xi)$ is a spatiotemporal moment-rate volume-density function of q^{th} basis component of moment tensor. While, q^{th} here corresponds to the degree of freedom of the moment rate tensor without isotropic expansion sources, and ξ symbolized a location in the source area.

In considering the inversion framework of Shimizu et al. (2020), we built a synthetic teleseismic waveform in the inversion process based on Green's function and the assumed source process model. Furthermore, we compared the synthetic waveform with the observed teleseismic waveform data for each worldwide recording station to justify that the source process model obtained by this study is relevant to its original state. A small error could indicate this. Eq. (2) shows how we built synthetic teleseismic waveforms for individual stations worldwide regarding the observed waveform data.

$$u_j(t) = \sum_{k=1}^{K}\sum_{l=1}^{L}\sum_{q=1}^{5} a_{qkl} \int_s \left(G_{qj}\,(t,\xi) + \delta G_{qj}\,(t,\xi)\right) * \left(X_k(\xi) T_l\,(t - tk)\right) d\xi + e_{bj}(t) \tag{2}$$

where u_j represents seismic waveform for far-field term observed at a station j by a linear combination of moment-rate volume-density functions of five basis components q^{th} of double couple moment tensor, K and L denote the slip direction on the model plane S, a_{qkl} are the expansion coefficients to be estimated from the observed data, $(G_{qj}\,(t,\xi) + \delta G_{qj}\,(t,\xi))$ is Green's function, X_k and T_l are the basis functions for space and time, respectively, and e_{bj} is a background and instrumental noise.

Furthermore, to perform a stable result, we applied a weighted moment tensor finite fault inversion method proposed by Yamashita et al. (2021). The smoothness constraints formulation used in Shimizu et al. (2020) is adjusting an identical Gaussian distribution for all basis components base on Akaike's Bayesian information criterion (Akaike, 1980). It possibly can bias the solution since the potency-rate density functions of basis components have a chance to experience a disproportionately smoothing compared to their amplitude. Potency density itself is referred to as a product of the average slip on a fault and the fault area, and potency-rate density is time variation of the potency density. However, by using the new method developed by Yamashita et al. (2021), we can adjust the standard deviation of the smoothing constraints proportionally with its magnitude for each basis double-couple component.

4. RESULTS AND DISCUSSION

We assessed the spatiotemporal distribution of the potency density tensor for the 2020 Bengkulu doublet earthquake by implementing the flexible finite-fault inversion method to teleseismic P waveforms. We employed a unique treatment in the inversion process by setting the same fault parameter with a strike of 321° and dip of 11° for the foreshock and mainshock by considering them as a doublet earthquake. Figure 2c and Figure 3a show that the fault has a length of 91 km along the strike and a width of 49 km along the dip direction. However, the rupture of the foreshock mainly occurred only in a limited area (red square) with a length of 49 km along the strike and 35 km along the dip direction. Furthermore, we found that there is only one asperity broke for each earthquake. The asperity of the foreshock is a little bit deeper and narrower than the mainshock, with the total maximum slip reached is 1.07 m. Meanwhile, the asperity of the mainshock is more comprehensive, with the total maximum slip reached is 1.17 m. The total moment tensor for both foreshock (Figure 2a) and mainshock (Figure 3c) shows a thrust fault mechanism corresponding to the subduction zone activity in southwestern Sumatra.

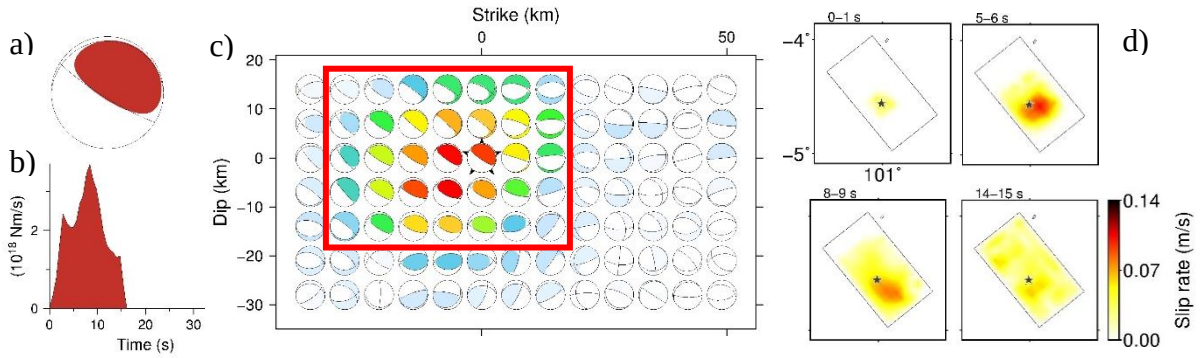

Figure 2. Inversion Result of the Foreshock. a) total moment tensor. b) source time function. c) total slip distribution. d) spatial-temporal rupture snapshot.

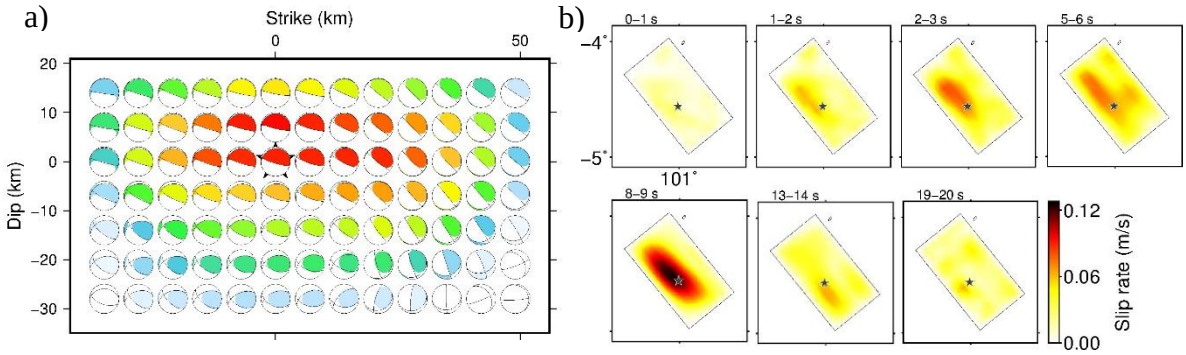

Figure 3. Inversion Result of the Mainshock. a) total slip distribution. b) spatial-temporal rupture snapshot. c) total moment tensor. d) source time function.

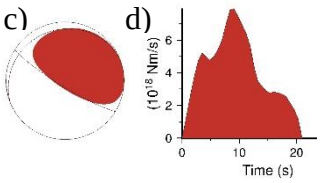

Moreover, by using the high degree of freedom finite fault inversion method, which allows us to extract the fault plane geometry information, we found that the dip angle along the fault plane changes with depth. If we look more closely at the shape of the focal mechanism from the shallow to the deep part of the fault plane, we can find that the dip angle increases with increasing depth. At the shallowest edge with a depth of 7.3 km, the initial dip angle starts from 7 degrees; then at a depth of 8.6 km, the dip angle becomes 9 degrees; at a depth of 10 km, the dip angle is 13 degrees; at a depth of 11.3 km, the dip angle is 20 degrees, respectively. As for the deeper parts, we cannot consider the dip angle because the slip generated in that area is relatively small.

In this study, we also set an exact hypocenter location for both foreshock and mainshock because we want to infer the new location of the mainshock hypocenter by referring to the location of the foreshock hypocenter considering that those are doublet earthquakes. The foreshock starts the rupture sequence of the doublet earthquake. The rupture duration of the foreshock is 15 seconds (Figure 2b), and it is started from the hypocenter (Figure 2d; black star). As the maximum rupture speed is set at 3.7 km/s, the foreshock rupture starts to expand circularly around the hypocenter and extends to the downdip direction. However, the propagation towards the deeper part is suspended at 5-6 seconds. Then, the rupture only extends in the shallower part in the southeastward direction from the hypocenter and reaches the peak moment release at 9 seconds (Figure 2b). Finally, the rupture ends at 15 seconds near the hypocenter (Figure 2d).

The mainshock then continues the doublet earthquake rupture sequence. In this study, we set the maximum rupture velocity of the mainshock as infinity because we want to infer the new location of the mainshock hypocenter. By doing this, all areas within the fault plane can break from the beginning. Then, we can identify the new location of the mainshock hypocenter by considering the high slip rate which occurs in the early seconds. Figure 3b shows that the high slip rate occurs at 1-2 seconds in the

west-northwestward from the foreshock hypocenter (black star). Therefore, we determined that such a location is the new mainshock hypocenter (blue star). If we pay attention, the mainshock hypocenter is established close to the termination area of the foreshock rupture. Consequently, we suppose that the foreshock rupture triggers the mainshock rupture. The mainshock rupture propagates northwestward until 3 seconds; then, it extends swiftly toward the deeper part until it is suspended at 6 seconds at the exact area where foreshock rupture was also suspended. After that, it only expands in the shallower part and reaches the peak moment release at 9 seconds (Figure 3d). Eventually, starting from the 13th second (Figure 3b), the series of rupture processes remains limited only in the southeastern part with consistent shrinkage until the 20th second, which is the expiration course of the mainshock earthquake source process (Figure 3d).

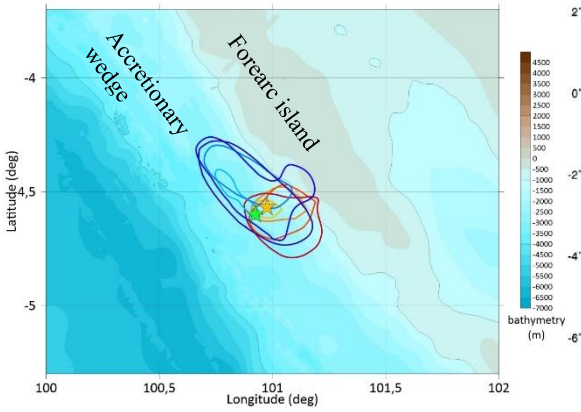

Figure 4. Map view of the doublet earthquake.

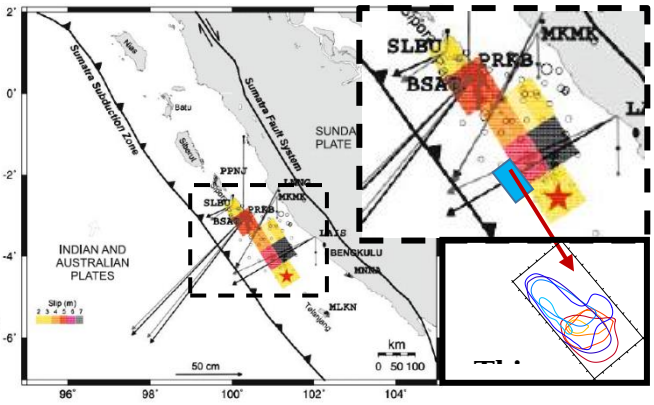

Figure 5. Slip distribution model of the 2007 Bengkulu earthquake (Mw 8.5) derived from the coseismic offset modelling at SuGAr GPS sites (modified from Ambikapathy et al., 2010).

Figure 4 shows the location of the foreshock hypocenter (orange star) and mainshock hypocenter (green star), including the 2020 Bengkulu doublet earthquake rupture sequence where orange polygons denote foreshock rupture snapshots and blue polygons represent mainshock rupture snapshot. If we look at the doublet earthquake fault plane scene by considering the bathymetry height, we can say that the doublet earthquake rupture occurred in the Sumatra forearc zone, specifically at the boundary between the accretion wedge (bluish contour) and the forearc island (brownish contour). Collings et al. (2012) discovered that the area beneath the forearc island has a different structure to the accretionary wedge closer to the trench. It is indicated by a higher Vp/Vs ratio under the forearc island, implying that the sediments in this area are more compressed and contain much less water which is squeezed during compaction. (Hyndman and Peacock, 2003).

Furthermore, Figure 5 is a slip distribution model for the 2007 Bengkulu earthquake (Mw 8.5) inferred from GPS data (Ambikapathy et al., 2010). we can find that the rupture of the doublet earthquake (blue rectangle) is located just southwestward of the 2007 Bengkulu earthquake asperity (reddish rectangle) location. We suspect that the structure discontinuity between the accretionary wedge and the forearc island is playing a role and becomes the reason why the foreshock and mainshock earthquake ruptures suspend when trying to extend toward deeper parts. Indeed, the structure contrast of the two regions also corresponds to the difference in rock stress capacity; hence that the 2020 Bengkulu doublet earthquake ruptures that occurred in a lower stress area was inadequate to trigger a break in the asperity area of the 2007 Bengkulu earthquake (Mw 8.5) which had higher stress capacity where the energy was already released during the 2007 Bengkulu earthquake.

5. CONCLUSIONS

This study investigated the source process of the 2020 Bengkulu doublet earthquake using the high degree of freedom finite fault inversion method recently developed by Shimizu et al. (2020) to the teleseismic bodywave data. We also applied several unique treatments in the inversion process, considering that the doublet earthquake has an adjacent location, time, and magnitude.

Accordingly, we found that the rupture in the fault plane was divided into two distinct areas between foreshock and mainshock indicated by the opposing location of two asperities. Furthermore, the movement pattern of the 2020 Bengkulu doublet earthquake rupture shows as if the mainshock earthquake continued the unfinished foreshock earthquake rupture but with a more comprehensive area coverage. In addition, we also suspect that the existence of a structure discontinuity located in the deepest part of the fault plane affects the cessation of the doublet earthquake rupture movement in that area. Moreover, using the high degree of freedom finite fault inversion method, which allows us to extract the fault plane geometry information, we discover that the dip angle changes along the fault plane as the depth increases.

ACKNOWLEDGEMENTS

This research was conducted during the individual study period of the training course “Seismology, Earthquake Engineering and Tsunami Disaster Mitigation” by the Building Research Institute, JICA, and GRIPS. I want to express my sincere gratitude to my supervisor Prof. Yuji Yagi for his valuable support and experience, which helped me to complete my research successfully. I would also like to acknowledge Dr. Bunichiro Shibazaki for his permanent support from the beginning to the end of the program.

REFERENCES

Akaike, H. (1980). Likelihood and the Bayes procedure. Trabajos de Estadistica Y de Investigacion Operativa. https://doi.org/10.1007/BF02888350

Ambikapathy, A., Catherine, J. K., Gahalaut, V. K., Narsaiah, M., Bansal, A., and Mahesh, P. (2010). The 2007 Bengkulu earthquake, its rupture model and implications for seismic hazard. Journal of Earth System Science. https://doi.org/10.1007/s12040-010-0037-2

Backus, G., & Mulcahy, M. (1976). Moment tensors and other phenomenological descriptions of seismic sources—II. Discontinuous displacements. Geophysical Journal of the Royal Astronomical Society. https://doi.org/10.1111/j.1365-246X.1976.tb01275.x

Bird, P. (2003). An updated digital model of plate boundaries. Geochemistry, Geophysics, Geosystems. https://doi.org/10.1029/2001GC000252

Kikuchi, M., & Kanamori, H. (1991). Inversion of complex body waves - III. Bulletin - Seismological Society of America.

Lay, T., and Kanamori, H. (1980). Earthquake doublets in the Solomon Islands. Physics of the Earth and Planetary Interiors. https://doi.org/10.1016/0031-9201(80)90134-X

Okuwaki, R., Hirano, S., Yagi, Y., and Shimizu, K. (2020). Inchworm-like source evolution through a geometrically complex fault fueled persistent supershear rupture during the 2018 Palu Indonesia earthquake. Earth and Planetary Science Letters. https://doi.org/10.1016/j.epsl.2020.116449

Shimizu, K., Yagi, Y., Okuwaki, R., and Fukahata, Y. (2020). Development of an inversion method to extract information on fault geometry from teleseismic data. Geophysical Journal International. https://doi.org/10.1093/gji/ggz496

Yamanaka, Y., and Kikuchi, M. (2003). Source process of the recurrent Tokachi-oki earthquake on September 26, 2003 inferred from teleseismic body waves. Earth, Planets and Space, 55(12). https://doi.org/10.1186/BF03352479

Yamashita, S., Yagi, Y., Okuwaki, R., Shimizu, K., Agata, R., and Fukahata, Y. (2021). Consecutive ruptures on a complex conjugate fault system during the 2018 Gulf of Alaska earthquake. Scientific Reports. https://doi.org/10.1038/s41598-021-85522-w